Progress In Electromagnetics Research, Vol. 149, 183–192, 2014

Compact Waveguided Metamaterials for Suppression of Mutual Coupling in Microstrip Array

Zeeshan Qamar and Hyun-Chang Park*

Abstract—In this paper, suppression of mutual coupling is achieved using compact waveguided metamaterials (WG-MTMs) in between elements of a densely packed microstrip array. Both the E-plane internally folded complementary split ring resonator and the H-plane internally folded complementary split ring resonator are employed to reduce the mutual coupling between adjacent elements. Coupling suppression of 18 dB and 9 dB, for elements in the E-plane and H-plane, respectively, is demonstrated. Due to the compact size of the waveguided metamaterials, the edge-to-edge separation between elements is kept at only $0.093\lambda_0$. With the same element spacing, a 2×2 array is also simulated with compact WG-MTMs. The proposed structure reduces the array size and enables the implementation of compact Multiple-Input-Multiple-Output systems.

1. INTRODUCTION

The microstrip antenna array in Multiple-Input-Multiple-Output (MIMO) applications is in limelight of the wireless world due to its compact size and ease of integration. For obtaining desirable isolation between antenna elements and for better performance, the traditional minimum spacing among array elements had to be one-half of the free-space wavelengths ($0.5\lambda_0$). Increasing demand for a compact terminal size in MIMO systems requires reduction in the array element spacing. However, this may cause deterioration in the performance of the antenna array due to the increased electromagnetic (EM) coupling among the closely packed antenna elements. Strong EM coupling results in the loss of the antenna efficiency and the bandwidth. It also degrades the diversity gain or the performance of the spatial multiplexing scheme [1].

Major sources of the EM coupling are the surface wave, space wave, and near-field coupling. Although surface waves are weakly excited in thin substrates, space waves dominantly increase the EM coupling when adjacent antennas are placed very close to each other [2]. The near-field coupling is also strong when antennas are printed on dielectric substrates with very low permittivity [3].

To reduce the mutual coupling, various types of electromagnetic band-gap (EBG) structures have been integrated in patch antenna arrays [4–7]. However, the design complexity and the large element spacing ($0.5\lambda_0$) of the array are the main concerns in these models. Defected ground structures (DGS) have been implemented by etching slots of different shapes in the ground plane of the antenna arrays [8]. However, this technique was employed only in the planar inverted-F antennas (PIFAs). Single negative (SNG) magnetic metamaterials have been used to reduce the mutual coupling between elements in a densely packed array [9]. The gap between the patches was $0.1\lambda_0$ with 20 dB isolation, but the design was very difficult to fabricate and restricted only for E-coupled elements array. WG-MTM has recently been proposed as a new category of effective medium [10, 11]. WG-MTM with crossed meander line slits has been designed which exhibits magnetic resonances [12]. Hilbert-shaped WG-MTM has been introduced to reduce the mutual coupling of closely packed elements [13]. In both structures, edge-to-edge element spacing was kept at $0.125\lambda_0$, but reduced coupling was achieved only in H-plane elements.

Received 30 June 2014, Accepted 14 October 2014, Scheduled 31 October 2014

* Corresponding author: Hyun Chang Park (hcpark@dongguk.edu).
The authors are with the Division of Electronics and Electrical Engineering, Dongguk University-Seoul, Seoul 100-715, Korea.

In this paper, two compact models of WG-MTM, E-plane internally folded complementary split ring resonator (E-IFCSRR) and H-plane internally folded complementary split ring resonator (H-IFCSRR), are proposed to mitigate the EM coupling between adjacent radiating elements in the E-plane and H-plane, respectively. There are two main reasons of introducing two different models, following the same design process. The first reason is to obtain the negative permittivity and negative permeability behaviors of E-IFCSRR and H-IFCSRR, respectively. The second reason is to integrate maximum number of cells in between the adjacent elements in both the E-coupled and the H-coupled cases. Hence, E-IFCSRR and H-IFCSRR occupy the same area, but they are rotated by 90 degrees with respect to each other to allow for co-existence in a two-dimensional patch array exhibiting uniform inter-element spacing. The proposed models occupy a very small area as compared to previous techniques. Due to their unique design as compared to previous WG-MTM structures, they eliminate the effect of two major sources of coupling which are the space wave and the near-field coupling. Moreover, the fabrication complexity is also much reduced as the proposed WG-MTMs are sandwiched between the adjacent elements in a planar waveguide environment. In the following, the proposed WG-MTM and their applications in a two-element microstrip array are presented. Measured results on the prototypes of the antenna array incorporating the proposed WG-MTMs are shown to validate the EM coupling suppression.

2. DESIGN METHODOLOGIES OF COMPACT WG-MTM STRUCTURES

WG-MTM is an artificial material made up of two parallel metal plates which are etched with patterns of periodical unit cells. These periodically etched unit cell plates, along with a volume (substrate) in between, constitute the effective medium with respect to the guided waves in the planar waveguide environment. These types of WG-MTMs are easy to fabricate with commercially available printed circuit board (PCB) process.

Compact WG-MTMs were designed on a Taconic substrate with relative permittivity of 2.2, thickness of 0.76 mm and loss tangent of 0.009. In order to study the scattering properties (reflection coefficient S_{11}, and transmission coefficient S_{21}), a quasi-transverse electromagnetic (TEM) waveguide setup was implemented in the commercially available EM solver HFSS 14 [13, 14] as depicted in Figure 1. Appropriate perfect electric conductor (PEC) and perfect magnetic conductor (PMC) boundaries were imposed in the z and x directions, respectively, to propagate the dominant TEM plane wave along y direction, with the electric field polarized perpendicular to, and the magnetic field parallel to, the periodical WG-MTMs. The upper part (copper) of WG-MTMs has been placed on the same surface where the antenna elements are located. The lower part has been integrated into the ground plane. Keeping these placements in mind, the substrate with the proposed structures has been simulated in unit cell modeling.

With the purpose of achieving band-stop characteristics at 2.45 GHz, compact WG-MTMs for both

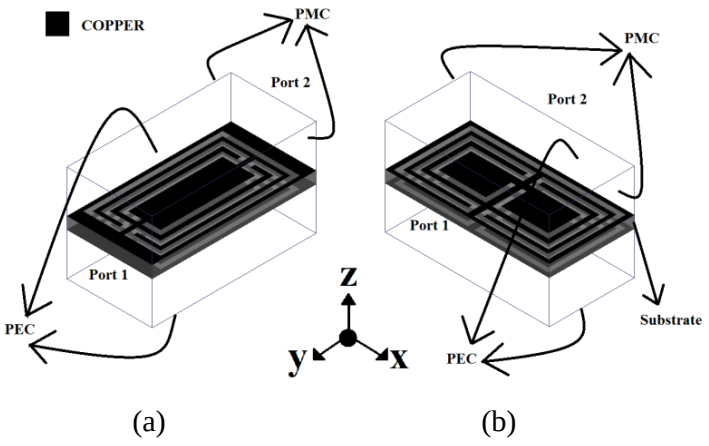

Figure 1. 3D view of (a) the E-coupled and (b) the H-coupled WG-MTM unit cells.

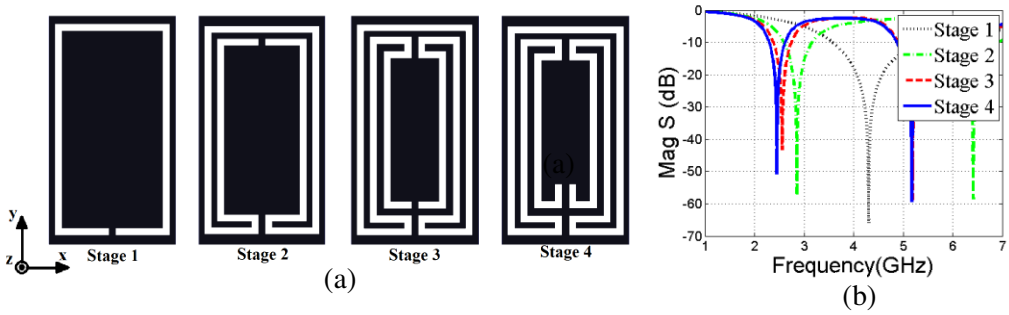

Figure 2. Design process of E-IFCSRR (a) geometric stages and (b) S-parameters (S_{21}).

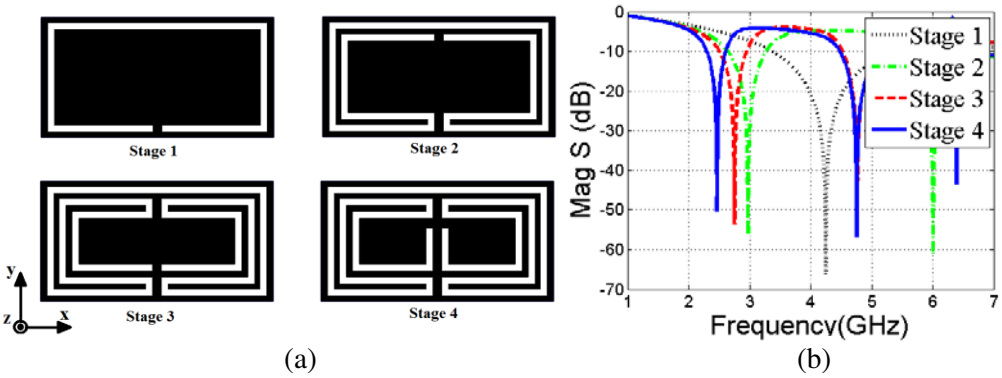

Figure 3. Design process of H-IFCSRR (a) geometric stages and (b) S-parameters (S_{21}).

the E- and H-planes were designed in successive stages as shown in Figure 2 and Figure 3, respectively.

In Stage 1, a single split ring called complementary split ring resonator (CSRR) was etched into the metal plates. The initial dimensions for this stage were obtained based on the method discussed by Shelby et al. [15] and further optimized to achieve decent band-stop characteristics. The frequency of the E-CSRR and H-CSRR was recorded as 4.3 GHz and 4.24 GHz, respectively. To lower the frequency of operation with the same unit cell size, another split ring was etched internally and connected with the outer ring using a slot in Stage 2. The resonant frequency was reduced to 2.85 GHz for E-IFCSRR and 2.98 GHz for H-IFCSRR. With the etching of another internal split ring in Stage 3, a slightly lower frequency was achieved as shown in Figures 2(b) and 3(b). In the last stage, instead of etching yet another split ring, two internal slots were introduced to get the desired frequency of operation at 2.45 GHz. The addition of two slots in the split section region of the innermost ring helped in fine-tuning the resonant frequency.

The final optimized structures and dimensions are depicted in Figure 4 and Table 1, respectively. The simulated responses of both models are shown in Figure 5. Scattering parameters of the WG-MTMs were obtained according to the literature [16–18]. To ascertain the negative permittivity and the negative permeability behavior of E-IFCSRR and H-IFCSRR, respectively, the constitutive parameters were also calculated using the technique given by Smith et al. [19]. Negative permittivity from 2.43 GHz to 2.53 GHz was observed in E-IFCSRR. Similarly, negative permeability was observed from 2.34 GHz to 2.56 GHz in H-IFCSRR. In order to achieve a structure with broadband characteristics, the use of multi-layered waveguided metamaterials is an interesting technique for future investigation [20].

Table 1. Optimized dimensions of the WG-MTMs.

Dimension	c	d	e	w	g	L	L_1	P	P_1
Value (mm)	1.65	0.74	0.3	0.3	0.3	10	10.6	5	5.5

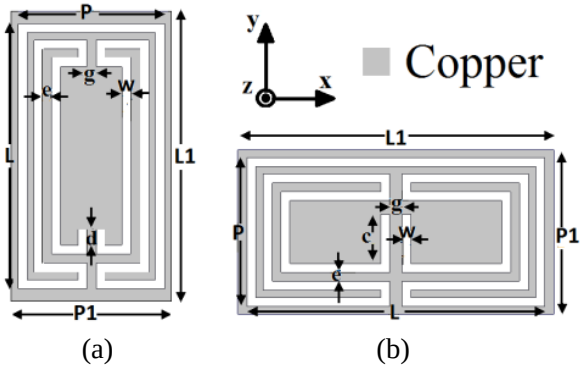

Figure 4. Geometry of WG-MTMs (a) E-IFCSRR and (b) H-IFCSRR.

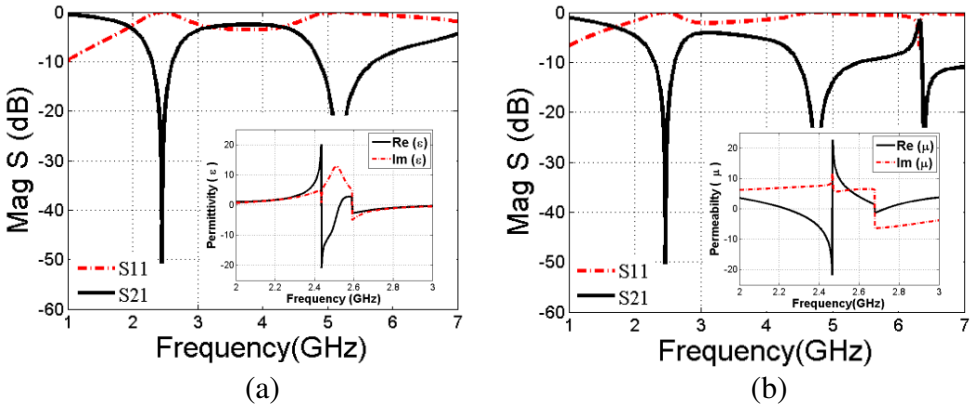

Figure 5. S-parameters along with constitutive parameters (a) E-IFCSRR and (b) H-IFCSRR.

3. APPLICATION OF WG-MTM IN MICROSTRIP ARRAYS

It is well known that near-field coupling and space waves significantly interrupt the adjacent elements of an array, both in the E- and H-planes. Therefore, two models of WG-MTMs have been introduced to suppress the EM coupling effect in both the E- and H-coupled array elements. The geometry of the microstrip arrays are shown in Figure 6, with $s = 0.422\lambda_0$ ($es = 0.093\lambda_0$). Table 2 contains the optimized dimensions of both arrays.

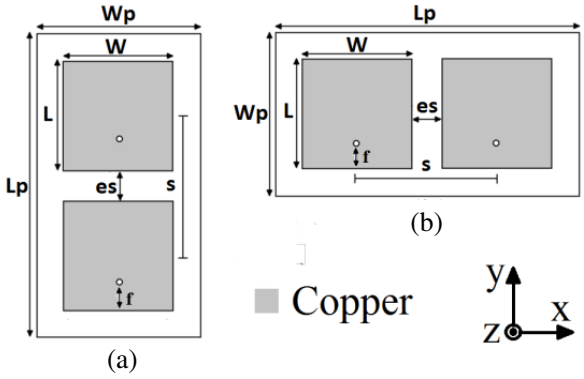

Figure 6. Geometric structure of the two-element arrays (a) E-coupled and (b) H-coupled.

Table 2. Physical parameters of the microstrip patch arrays.

Dimension	L_p	W_p	W	L	es	s	f
Value (mm)	111.7	60	40.34	40.34	11.36	51.7	14.37

WG-MTMs (E-IFCSRR or H-IFCSRR) were sandwiched between the array elements on both sides of the substrate as shown in Figure 7, to suppress the surface waves propagating on the air-dielectric interface along y-axis for the E-coupled and x-axis for the H-coupled arrays. The space waves, which are responsible for enhanced coupling, are also suppressed by the WG-MTMs, as they capture and convert the space waves to the surface current.

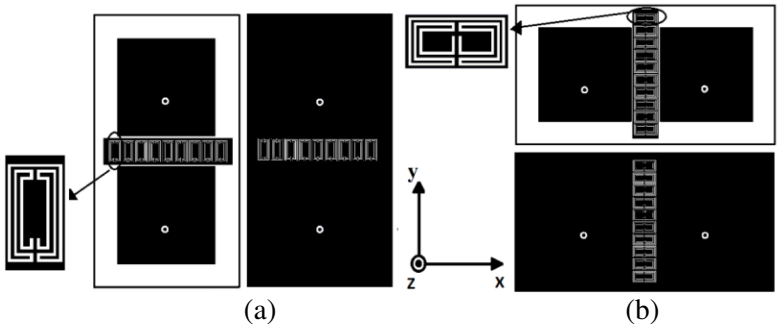

Figure 7. Top and bottom view of the two-element arrays with WG-MTMs (a) E-coupled and (b) H-coupled.

When the E-IFCSRR was placed in between the E-coupled elements, a slight shift of 19 MHz was observed in the resonant frequency. This is because the decoupling structures and patch antennas are in a proximity which produces the slow-wave effect and disturbs the impedance matching, resulting in the frequency shift from 2.427 GHz to 2.446 GHz [21]. The mutual coupling has drastically reduced from −16 dB to −34 dB, as shown in Figure 8(a). Therefore, coupling suppression of 18 dB has been calculated for the proposed E-IFCSRR antenna.

Unlike the E-coupled array, no shift in the resonant frequency was witnessed when the H-IFCSRR was placed in between the H-coupled elements. This is due to the placement of WG-MTMs along the non-resonant edges of the patch where the slow-wave effect is less dominant than observed in the E-coupled elements. Significant reduction in the mutual coupling, from −13 dB to −22 dB, is marked as shown in Figure 8(b). Hence, 9 dB mutual coupling reduction has been realized for the proposed H-IFCSRR antenna.

To further investigate the suppression attributes, the surface current distribution on the patches and the ground plane is plotted together and shown in Figure 9 as a single snapshot. The plots are created by exciting one element and terminating the other element with 50 ohm matched load. The coupling current on the ground plane caused by surface waves and space waves is progressively confined when the WG-MTMs are included in the array.

4. EXPERIMENTAL RESULTS AND VERIFICATION

The fabricated microstrip patch arrays (MPAs) with WG-MTMs, as shown in Figure 10, were measured using Agilent N5242A PNA-X network analyzer. As observed in Figure 11, a very adequate impedance matching and negligible frequency shift have been observed in both cases. For the E-coupled array, return loss (S_{11}) as low as −34 dB has been measured. In the case of the H-coupled array, S_{11} of −23 dB has been recorded. The mutual coupling (S_{21}) has been suppressed down to −33 dB and −22 dB for the E-coupled and the H-coupled antenna arrays, respectively.

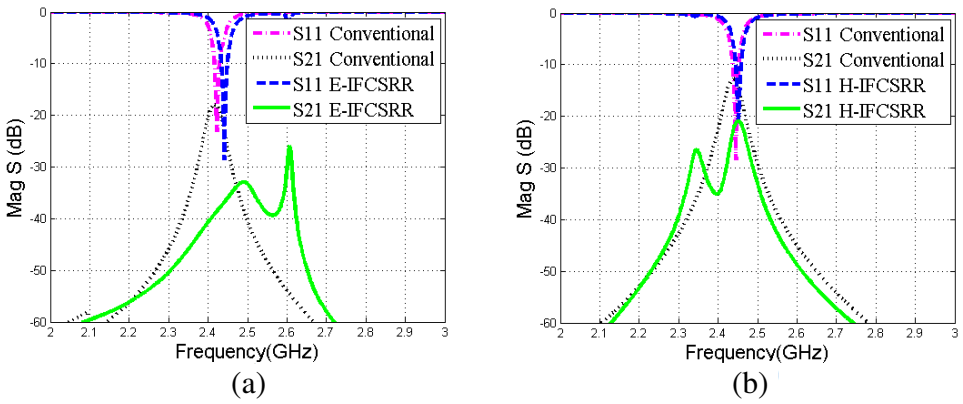

Figure 8. *S*-parameters of the two-element array (a) E-coupled and (b) H-coupled.

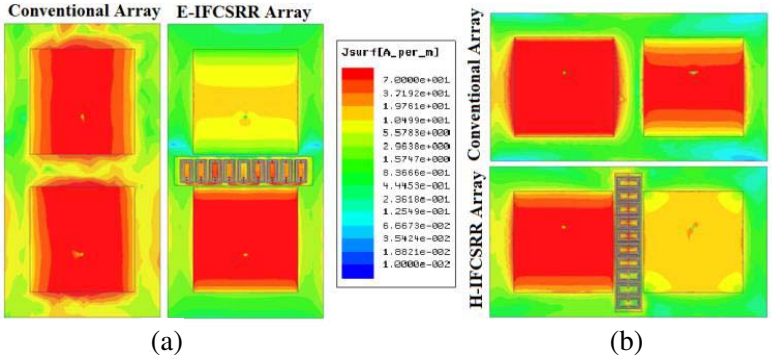

Figure 9. Snapshot for surface current in the patches and the ground planes of (a) E-coupled and (b) H-coupled arrays.

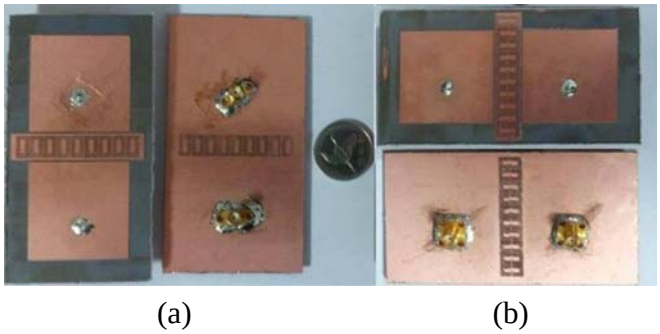

Figure 10. Top and bottom view of (a) the E-coupled and (b) the H-coupled prototypes.

The radiation pattern of the demonstrated MPAs was measured by exciting one element of the array and terminating the other element with a 50 ohm matching load. Figure 12 shows the simulated and the measured radiation characteristics in the *E*- and *H*-planes of the E-coupled array with and without E-IFCSRR. The measured gain is 5.92 dB. In a similar manner, Figure 13 contains the simulated and the measured radiation characteristics in the *E*- and *H*-planes of the H-coupled array with and without H-IFCSRR. The measured gain is 6.02 dB. Although a minute influence on the antenna radiation characteristics such as gain and front-to-back ratio is observed, the radiation patterns do not show any significant difference between the main lobes.

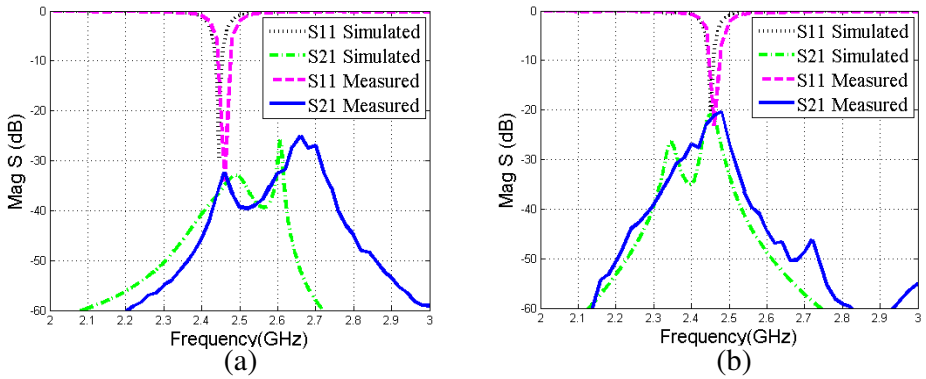

Figure 11. Simulated and measured S-parameters of arrays with WG-MTMs (a) E-coupled and (b) H-coupled.

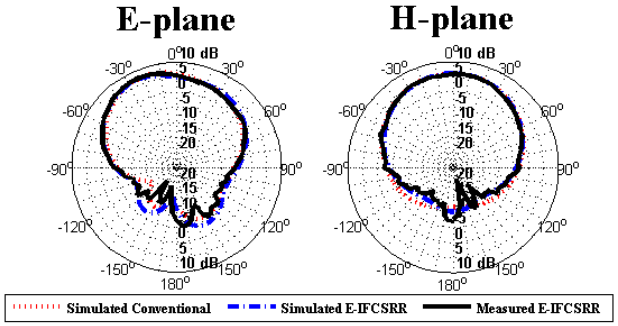

Figure 12. Simulated and measured radiation patterns of the E-coupled array in the E- and the H-planes.

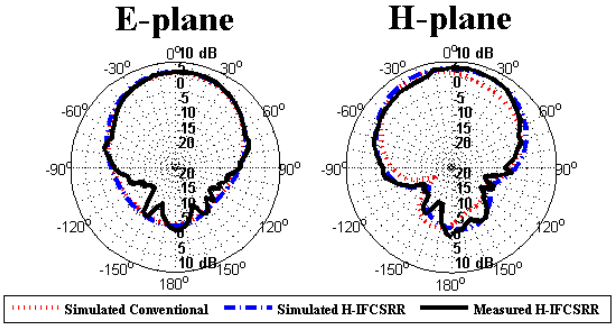

Figure 13. Simulated and measured radiation patterns of the H-coupled array in the E- and the H-planes.

5. SIMULATION RESULTS FOR 2 × 2 ARRAY

The proposed WG-MTMs were also placed in between the adjacent elements of a 2×2 array, as shown in Figure 14. The spacing between the elements is the same ($es = 11.36\,\text{mm}$) as that of the E-coupled

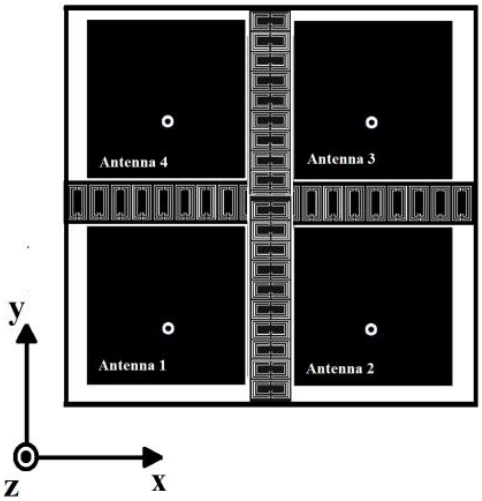

Figure 14. Top view of a 2×2 array with compact WG-MTMs.

and H-coupled arrays already mentioned in Section 3. The total length of the periodic WG-MTMs is 104.5 mm by placing 19 unit cells in between elements of the 2×2 array. Hence, WG-MTMs are extended by 6.23 mm on each side of the patch antenna footprint in order to achieve a compact 2D array size of $104.5 \times 104.5\,\text{mm}^2$. As depicted in Figure 15(a), slight shift in frequency has been observed after introducing the WG-MTMs in between all the elements of the 2×2 array. On the other hand, enhanced coupling suppression among the elements has been observed. As shown in Figures 15(b)–(d), coupling suppressions of $S_{21} = 9.8\,\text{dB}$, $S_{31} = 20\,\text{dB}$ and $S_{41} = 16\,\text{dB}$ are recorded. The simulated radiation patterns for E- and H-planes are demonstrated in Figure 16. As noted earlier, the radiation patterns do not show any significant difference between the main lobes, although minute influence on the antenna radiation characteristics is observed.

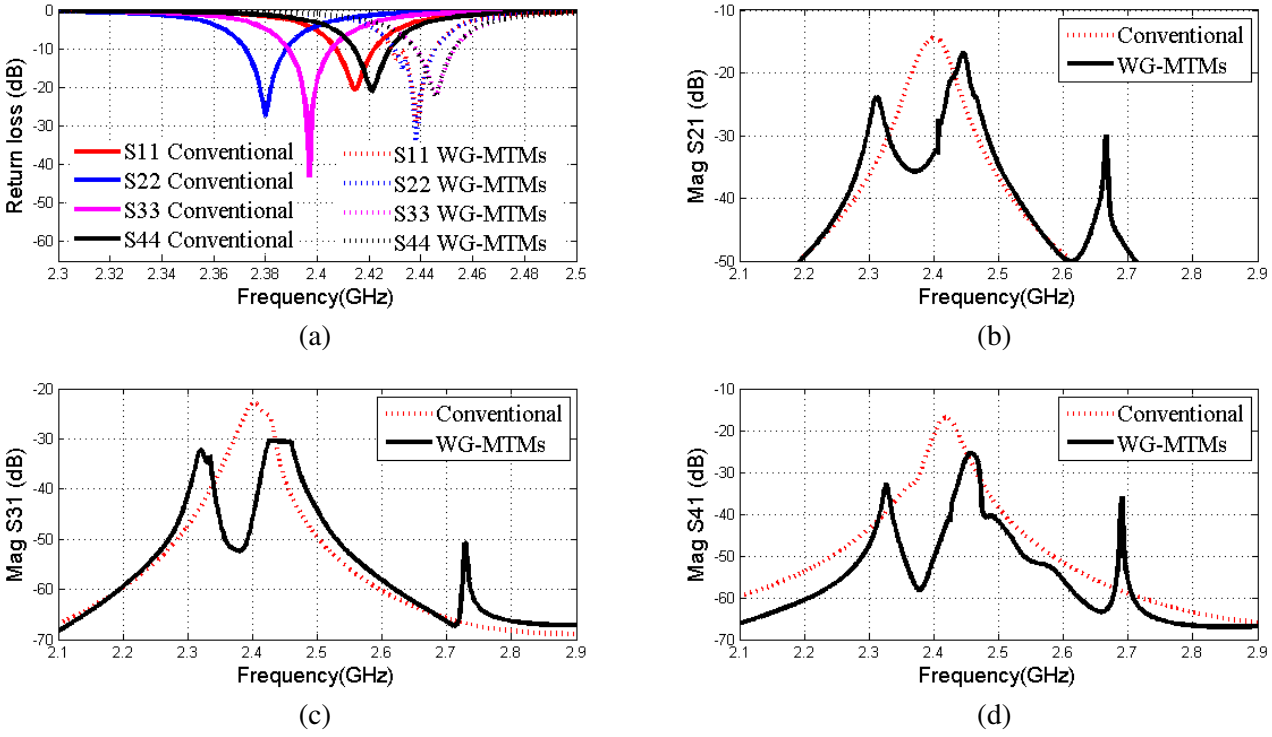

Figure 15. Simulated S-parameters of the 2×2 array. (a) Return loss. (b) Mutual coupling between antenna 2 and antenna 1 (S_{21}). (c) Mutual coupling between antenna 3 and antenna 1 (S_{31}). (d) Mutual coupling between antenna 4 and antenna 1 (S_{41}).

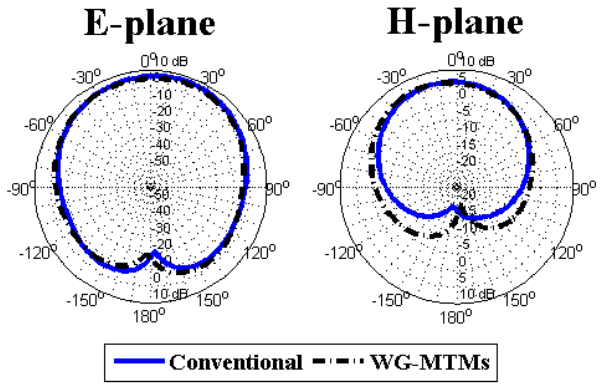

Figure 16. Simulated radiation patterns of the 2×2 array in the E- and the H-planes.

6. CONCLUSION

Compact WG-MTMs have been demonstrated for the mutual coupling suppression in densely packed arrays with edge separation of only $0.093\lambda_0$. Two types of WG MTMs, i.e., E-IFCSRR and H-IFCSRR, are sandwiched in between the E- and H-coupled radiating elements, respectively. Measured mutual coupling is recorded to be nearly -33 dB for the E-coupled array, and -22 dB for the H-coupled array. The measured radiation patterns show very close correspondence with the simulated results. WG-MTMs have also been implemented in a 2×2 array, and their simulated results are presented. The demonstrated design can be easily fabricated and may be used in many compact Multiple-Input Multiple-Output (MIMO) applications.

REFERENCES

1. Ludwig, A., "Mutual coupling, gain and directivity of an array of two identical antennas," *IEEE Transaction on Antennas and Propagation*, Vol. 24, No. 6, 837–841, 1976.
2. Bait-Suwailam, M. M., O. F. Siddiqui, and O. M. Ramahi, "Mutual coupling reduction between microstrip patch antennas using slotted-complementary split-ring resonators," *IEEE Antennas and Wireless Propagation Letter,* Vol. 9, 876–878, 2010.
3. Nikolic, M., A. Djordjevic, and A. Neorai, "Microstrip antennas with suppressed radiation in horizontal directions and reduced coupling," *IEEE Transaction on Antennas and Propagation,* Vol. 52, No. 11, 3469–3476, 2005.
4. Yang, F. and Y. Rahmat-Samii, "Microstrip antennas integrated with electromagnetic band-gap (EBG) structures: A low mutual coupling design for array applications," *IEEE Transaction on Antennas and Propagation*, Vol. 51, No. 10, 2936–2946, 2003.
5. Coulombe, M., S. F. Koodiani, and C. Caloz, "Compact elongated mushroom (EM)-EBG structure for enhancement of patch antenna array performances," *IEEE Transaction on Antennas and Propagation*, Vol. 58, No. 4, 1076–1086, 2010.
6. Assimonis, S. D., V. Y. Traianos, and S. A. Christos, "Computational investigation and design of planar EBG structures for coupling reduction in antenna applications," *IEEE Transaction on Magnetics,* Vol. 48, No. 2, 771–774, 2012.
7. Farahani, H. S., M. Veysi, M. Kamyab, and A. Tadjalli, "Mutual coupling reduction in patch antenna arrays using a UC-EBG superstrate," *IEEE Antennas and Wireless Propagation Letter,* Vol. 9, 57–59, 2010.
8. Chiu, C. Y., C. H. Cheng, R. D. Murch, and C. R. Rowell, "Reduction of mutual coupling between closely-packed antenna elements," *IEEE Transaction on Antennas and Propagation,* Vol. 55, No. 6, 1732–1738, 2007.
9. Buell, K., H. Mosallaei, and K. Sarabandi, "Metamaterial insulator enabled superdirective array," *IEEE Transaction on Antennas and Propagation,* Vol. 55, No. 4, 1074–1085, 2007.
10. Liu, R., X. M. Yang, J. G. Gollub, J. J. Mock, T. J. Cui, and D. R. Smith, "Gradient index circuit by waveguided metamaterials," *Applied Physics Letter*, Vol. 94, No. 7, 073506, 2009.
11. Yang, X. M., Q. H. Sun, Y. Jing, Q. Cheng, X. Y. Zhou, H. W. Kong, and T. J. Cui, "Increasing the bandwidth of microstrip patch antenna by loading compact artificial magneto-dielectrics," *IEEE Transaction on Antennas and Propagation*, Vol. 59, No. 2, 373–378, 2011.
12. Yang, X. M., X. G. Liu, X. Y. Zhou, and T. J. Cui, "Reduction of mutual coupling between closely packed patch antennas using waveguided metamaterials," *IEEE Antennas and Wireless Propagation Letter*, Vol. 11, 389–391, 2012.
13. Han, X., H. Hafdallah Ouslimani, T. Zhang, and A. C. Priou, "CSRRS for efficient reduction of the electromagnetic interferences and mutual coupling in microstrip circuits," *Progress In Electromagnetics Research B*, Vol. 42, 291–309, 2012.
14. Xu, H. X., G. M. Wang, and M. Q. Qi, "Hilbert-shaped magnetic waveguided metamaterials for electromagnetic coupling reduction of microstrip antenna array," *IEEE Transaction on Magnetics*, Vol. 49, No. 4, 1526–1529, 2013.

15. Shelby, R. A., D. R. Smith, and S. Schultz, "Experimental verification of a negative index of refraction," *Science*, Vol. 292, No. 5514, 77–79, 2001.
16. Schurig, D., J. J. Mock, and D. R. Smith, "Electric-field coupled resonators for negative permittivity metamaterials," *Applied Physics Letter*, Vol. 88, 041109, 2006.
17. Wu, Q., P. Pan, F. Y. Meng, L. W. Li, and I. Wu, "A novel flat lens horn antenna designed based on zero refraction principle of metamaterials," *Applied Physics A*, Vol. 87, No. 2, 151–156, 2007.
18. Smith, D. R., J. GolIub, J. J. Mock, W. J. Padila, and D. Schurig, "Calculation and measurement of bianisotropy in a split ring resonator metamaterial," *Journal of Applied Physics*, Vol. 100, No. 19, 024507, 2006.
19. Smith, D. R., S. Schultz, P. Markos, and C. M. Soukoulis, "Determination of negative permittivity and permeability of materials from reflection and transmission coefficients," *Physics Rev. B*, Vol. 65, 195104, 2002.
20. Gu, S., J. P. Barrett, T. H. Hand, B. I. Popa, and S. A. Cummer, "A broadband low-reflection metamaterial absorber," *Journal of Applied Physics*, Vol. 108, No. 6, 064913, 2010.
21. Hou, D. B., S. Xiao, B.-Z. Wang, L. Jiang, J. Wang, and W. Hong, "Elimination of scan blindness with compact defected ground structures in microstrip phased array," *IET Microwaves, Antennas and Propagation*, Vol. 3, No. 2, 269–275, 2009.